Anal Bioanal Chem (2014) 406:4663–4675
DOI 10.1007/s00216-014-7870-0

RESEARCH PAPER

Development and validation of a LC-MS/MS assay for quantitation of plasma citrulline for application to animal models of the acute radiation syndrome across multiple species

Jace W. Jones · Gregory Tudor · Alexander Bennett · Ann M. Farese · Maria Moroni · Catherine Booth · Thomas J. MacVittie · Maureen A. Kane

Received: 25 March 2014 / Revised: 24 April 2014 / Accepted: 29 April 2014 / Published online: 20 May 2014

Abstract The potential risk of a radiological catastrophe highlights the need for identifying and validating potential biomarkers that accurately predict radiation-induced organ damage. A key target organ that is acutely sensitive to the effects of irradiation is the gastrointestinal (GI) tract, referred to as the GI acute radiation syndrome (GI-ARS). Recently, citrulline has been identified as a potential circulating biomarker for radiation-induced GI damage. Prior to biologically validating citrulline as a biomarker for radiation-induced GI injury, there is the important task of developing and validating a quantitation assay for citrulline detection within the radiation animal models used for biomarker validation. Herein, we describe the analytical development and validation of citrulline detection using a liquid chromatography tandem mass spectrometry assay that incorporates stable-label isotope internal standards. Analytical validation for specificity, linearity, lower limit of quantitation, accuracy, intra- and interday precision, extraction recovery, matrix effects, and stability was performed under sample collection and storage conditions according to the Guidance for Industry, Bioanalytical Methods Validation issued by the US Food and Drug Administration. In addition, the method was biologically validated using plasma from well-characterized mouse, minipig, and nonhuman primate GI-ARS models. The results demonstrated that circulating citrulline can be confidently quantified from plasma. Additionally, circulating citrulline displayed a time-dependent response for radiological doses covering GI-ARS across multiple species.

Keywords Citrulline · LC-MS/MS · Biomarker validation · Plasma biomarkers · Acute radiation syndrome · Radiation animal models

Electronic supplementary material The online version of this article (doi:10.1007/s00216-014-7870-0) contains supplementary material, which is available to authorized users.

J. W. Jones
Department of Pharmaceutical Sciences, School of Pharmacy, University of Maryland, Baltimore, 20 N. Pine Street, Room 721N, Baltimore, MD 21201, USA

G. Tudor · C. Booth
Epistem Ltd, 48 Grafton St, Manchester M13 9XX, UK

A. Bennett · A. M. Farese · T. J. MacVittie
Department of Radiation Oncology, School of Medicine, University of Maryland, 655 W. Baltimore Street, Baltimore, MD 21201, USA

M. Moroni
Radiation Countermeasures Program, Armed Forces Radiobiology Research Institute, Uniformed Services University of the Health Sciences, 8901 Wisconsin Avenue, Building 42, Bethesda, MD 20889-5603, USA

M. A. Kane (✉)
Department of Pharmaceutical Sciences, School of Pharmacy, University of Maryland, Baltimore, 20 N. Pine Street, Room 723N, Baltimore, MD 21201, USA
e-mail: mkane@rx.umaryland.edu

Introduction

The potential threat of radiological disasters, be it accidental or deliberate, carry the risk of widespread high-dose radiation injury. Such injuries are classified as acute radiation syndrome (ARS) and delayed effects of acute radiation exposure (DEARE) [1]. One particular target associated with ARS is the gastrointestinal (GI) tract, specifically the small intestine. The small intestine is acutely sensitive to radiological exposure due to its rapidly proliferating epithelium and incapacity to efficiently repair DNA damage [2]. As such, circulating biomarkers indicative of small intestine function and integrity provide great promise in predicting (i.e., prognostic

biomarkers) and identifying (i.e., diagnostic biomarkers) radiation injury associated with the acute GI-ARS.

Changes in circulating citrulline levels have been suggested to predict small intestine tissue damage. Reduced citrulline has been shown to reflect small intestinal damage following chemotherapy [3] and radiotherapy [4] of the small bowel. In addition, citrulline has been associated with diagnostic monitoring following small bowel transplantation [5], enterocyte mass assessment in villous atrophy disease [6], Crohn's disease [3], enterocyte functional mass in HIV patients [7], and gut permeability following ethanol exposure [8].

Citrulline, a non-DNA encoded amino acid, is found as a circulating metabolite in blood plasma and other physiological fluids including urine, cerebrospinal fluid, amniotic fluid, and sweat [9]. Citrulline metabolism is linked to three important metabolic pathways: transformation of ammonia to urea in the liver, synthesis of arginine from glutamine in the GI tract and kidneys, and nitric oxide synthesis [9]. The biosynthesis of citrulline originates almost exclusively in small intestine enterocytes [10]. It is this process where citrulline is predominately formed in the small bowel enterocytes that tethers circulating citrulline to small intestine function.

The analysis of citrulline and amino acids in general has been accomplished by a variety of analytical techniques [11–16]. Of note, the use of liquid chromatography tandem mass spectrometry (LC-MS/MS) for amino acid quantitation is an efficient, reliable, and robust method owning to its selectivity and sensitivity [17–21]. Recently, several reports have demonstrated the effectiveness of citrulline quantitation from blood plasma using a LC-MS/MS platform [22–28]. These methods take advantage of the use of hydrophilic interaction liquid chromatography (HILIC) coupled to tandem mass spectrometry detection via selected reaction monitoring (SRM). HILIC column chemistry provides normal phase separating effectiveness for polar compounds (e.g., amino acids) while combining the use of high organic solvents in the mobile phase for enhancing ionization and desolvation of analytes [19, 29]. The net effect is traditional derivatization steps or ion-pairing type separations used for amino acid separation are not necessary. Thus, amino acids, in particular citrulline, quantitation can be achieved with high selectivity and sensitivity using the combined effort of HILIC separation and SRM detection.

We report the method development and validation for quantitation of citrulline from blood plasma from well-defined animal models of acute radiation effects in the GI-ARS dose range using LC-MS/MS firmly adhering to the Federal Drug Administration (FDA) Guidance for Industry, Bioanalytical Methods Validation [30]. Development and validation of this method, especially with the use of well-characterized animal models, is immensely important for determining the potential use of citrulline as a biomarker for GI-ARS. Because the conduct of human radiation experiments is unethical, the use of the nonhuman animal models is the only accepted pipeline for development and eventual FDA approval of medical countermeasures (MCMs) to treat high-dose irradiation injuries. A vital aspect of developing drug development tools, such as MCMs, is the identification and validation of biomarkers that can be used as quantitative measures for MCM efficacy. Therefore, it is essential to establish a validated analytical method for determination of citrulline from blood plasma using the same radiation animal models that are used for the drug development tools. Particular attention was devoted towards determining the most selective and sensitive SRM transitions in addition to determining the most appropriate quantitation method within the context of using blood plasma from radiation animal models. To date, systematic evaluation of multiple citrulline SRM transitions including the three most abundant *m/z* transitions (*m/z* 176→159, 176→113, and 176→70) found in literature has not been reported. In addition, the choice of citrulline quantitation using neat standards, background subtraction, or the surrogate analyte approach has not been documented for citrulline quantitation from blood plasma on a tandem quadrupole mass spectrometer. Herein, we detail the choice for selecting the most appropriate SRM transition and quantitation method for plasma citrulline measurements from radiation animal models. Following analytical validation, this assay was successfully applied to the analysis of plasma from mouse, minipig, and nonhuman primate (NHP) models that were exposed to radiological doses covering the acute GI-ARS.

Experimental

Chemicals and reagents L-citrulline (Cit) and L-arginine (Arg) were purchased from Sigma Aldrich (St. Louis, MO). 4,4,5,5-d_4-L-citrulline (d_4-Cit), 5-^{13}c-4,4,5,5-d_4-L-citrulline (^{13}c-d_4-Cit), and ^{13}c-L-citruline (^{13}c-Cit) were purchased from Cambridge Isotope Laboratories (Tewksbury, MA). The stable-label isotope standards were certified by Cambridge Isotope Laboratories at 95 % for d_4-Cit, 99 and 95 % for ^{13}c-d_4-Cit, and 99 % for ^{13}c-Cit. The stable-label isotope standards were used as received. d_4-Cit was used as the internal standard for the stable-label isotope methods. ^{13}c-Cit was used for the analyte surrogate and ^{13}c-d_4-Cit as the internal standard for the quantitation method via the analyte surrogate approach method. Optima LC-MS grade water (H_2O), acetonitrile (ACN), ammonium formate, and formic acid (FA) were purchased from Fisher Scientific (Pittsburg, PA). All chemicals and reagents were used without further purification.

Plasma samples Donated human plasma samples were obtained from the University of Maryland, Medical Center

Blood Bank (Baltimore, MD). Mouse plasma samples were obtained from Epistem Laboratories Ltd (Manchester, UK). NHP plasma samples were provided by the laboratory of Dr. Thomas J. Macvittie, University of Maryland, School of Medicine, Department of Radiation Oncology (Baltimore, MD). Minipig plasma samples were obtained from the laboratory of Dr. Maria Moroni, Armed Forces Radiobiology Research Institute (Bethesda, MD). Descriptions of the animal models including radiation exposure and dosimetry, medical management (supportive care and health status monitoring), and generation of plasma have been previously described [31–33].

Calibration standards For the stable-label isotope method, stock solutions of Arg, Cit, and d_4-Cit were prepared in H_2O/ACN (1:1, *v*/*v*) with 0.1 % FA. Calibration standards ranging from 0.1 to 200 μM of Cit with spiked amounts of 10 μM d_4-Cit (internal standard) and 200 μM of Arg were prepared in neat solution (H_2O:ACN (1:1, *v*/*v*) with 0.1 % FA). Human, mouse, and NHP plasma samples were spiked with Cit at concentrations ranging from 1.0 to 200 μM and d_4-Cit at 10 μM. Quality control samples at three concentration levels (5, 50, and 100 μM) were also prepared for neat standards and plasma samples. For the analyte surrogate method, stock solutions of Arg, ^{13}c-Cit, and ^{13}c-d_4-Cit were prepared in H_2O/ACN (1:1, *v*/*v*) with 0.1 % FA. Calibration standards ranging from 0.1 to 200 μM of ^{13}c-Cit with spiked amounts of 10 μM ^{13}c-d_4-Cit (internal standard) and 200 μM of Arg were prepared in neat solution (H_2O/ACN (1:1, *v*/*v*) with 0.1 % FA). Human, mouse, and NHP plasma samples were spiked with ^{13}c-Cit at concentrations ranging from 1.0 to 200 μM and d_4-Cit at 10 μM. Quality control samples at three concentration levels (5, 50, and 100 μM) were also prepared for neat standards and plasma samples.

Sample preparation Plasma samples were prepared as follows. 50 μL of plasma was combined with 10 μM of d_4-Cit (or ^{13}c-d_4-Cit) and 500 μL of ACN for protein precipitation. The mixture was thoroughly mixed for 30 s followed by centrifugation at 12,000 rpm for 10 min; 500 μL of supernatant was transferred and dried under a steady stream of nitrogen. Next, the sample was resuspended in H_2O/ACN (1:1, *v*/*v*) with 0.1 % FA and ready for analysis.

Liquid chromatography tandem mass spectrometry conditions LC-MS/MS analysis was performed on a TSQ Quantum Ultra Triple Stage Quadrupole Mass Spectrometer coupled to an Ultimate 3000 RS Liquid Chromatogram system (Thermo Scientific, San Jose, CA). The LC separation was performed on a Kinetex HILIC 100A column (4.6×100 mm, 2.6 μm) (Phenomenex, Torrance, CA) operated at 30 °C. Solvent A and B consisted of 10 mM ammonium formate with 0.1 % FA in water and ACN with 0.1 % FA, respectively. The gradient program was 0.0–0.5 min, 70 % B; 0.5–1.0 min, gradient to 10 % B; 1.0–3.5 min, 10 % B; 3.5–4.0 min, gradient to 70 % B; and 4.0–6.0 min, 70 % B. The flow rate was to 0.6 mL/min during all separation steps and injection volume was 10 μL.

Detection was performed in the positive-ion mode and the electrospray ionization (ESI) source parameters were as follows: spray voltage, 3,000; capillary temperature, 325; sheath gas pressure, 60; ion sweep gas pressure, 0.2; capillary offset, 10; and tube lens offset, 50–75. Data collection and analysis was performed by Xcalibur V 2.1 (Thermo Scientific, San Jose, CA) and Prism 6 (Graph Pad, La Jolla, CA).

Method validation The method was validated for specificity, linearity, lower limit of quantitation (LLOQ), accuracy, intra- and interday precision, extraction recovery, matrix effects, and stability under sample collection and storage according to the Guidance for Industry, Bioanalytical Methods Validation issued by the Food and Drug Administration (FDA) [30].

Statistics Statistical analyses were performed using GraphPad Prism 6.0 software (GraphPad Software Inc., La Jolla, USA).

Results

Mass spectrometry detection The mass spectrometry parameters for detection and quantitation for Cit from plasma are listed in Table 1 and representative mass spectra are shown in Fig. 1. The ESI mass spectra of Cit, d_4-Cit, and Arg displayed abundant protonated ions at *m/z* values of 176.1, 180.1, and 175.1, respectively. In addition, abundant ions at *m/z* values 159.1 and 163.1 were present corresponding to the neutral loss of ammonia (NH_3) from the protonated precursor ions at *m/z* 176.1 (Cit) and *m/z* 180.1 (d_4-Cit). These abundant neutral loss precursor ions highlight the ease at which the amino functional group dissociates from the intact Cit and d_4-Cit gas-phase ions. Ionization conditions including spray voltage, capillary temperature, and tube lens offset were optimized to maximize the signal intensity of the SRM transitions of choice. A consequence of this approach yielded a full scan mass spectrum (Fig. 1a) where abundant neutral loss product ions ($[M\text{-}NH_3+H]^+$) were present. Ideal ionization conditions result in little to no fragmentation of the precursor ion and therefore we proceeded to optimize the ionization conditions to minimize precursor ion fragmentation. Efforts to reduce the formation of the $[M-NH_3+H]^+$ product ion corresponded to reduced signal intensity on the SRM transitions (data not shown). Ultimately, we justified our ionization conditions based on total ion intensity of the SRM transitions and not on the precursor to product ion intensity ratios from the full-

Table 1 Mass spectrometry parameters for detection and quantitation for Cit, d_4-Cit, and Arg from plasma samples

Analyte	SRM transition (*m/z*)	Retention time (t_r; min)	Electrospray voltage (V)	Collisional energy (V)	Tube lens offset (V)	Collisional gas pressure (mTorr)
Cit	176.1→70.1	3.12	3,000	23	75	1.3
	176.1→159.1	3.12	3,000	5	50	1.3
d_4-Cit (IS)	180.1→74.1	3.12	3,000	23	75	1.3
Arg	175.1→70.1	3.30	3,000	23	75	1.3

d_4-Cit was used as the stable-label isotope internal standard (IS)

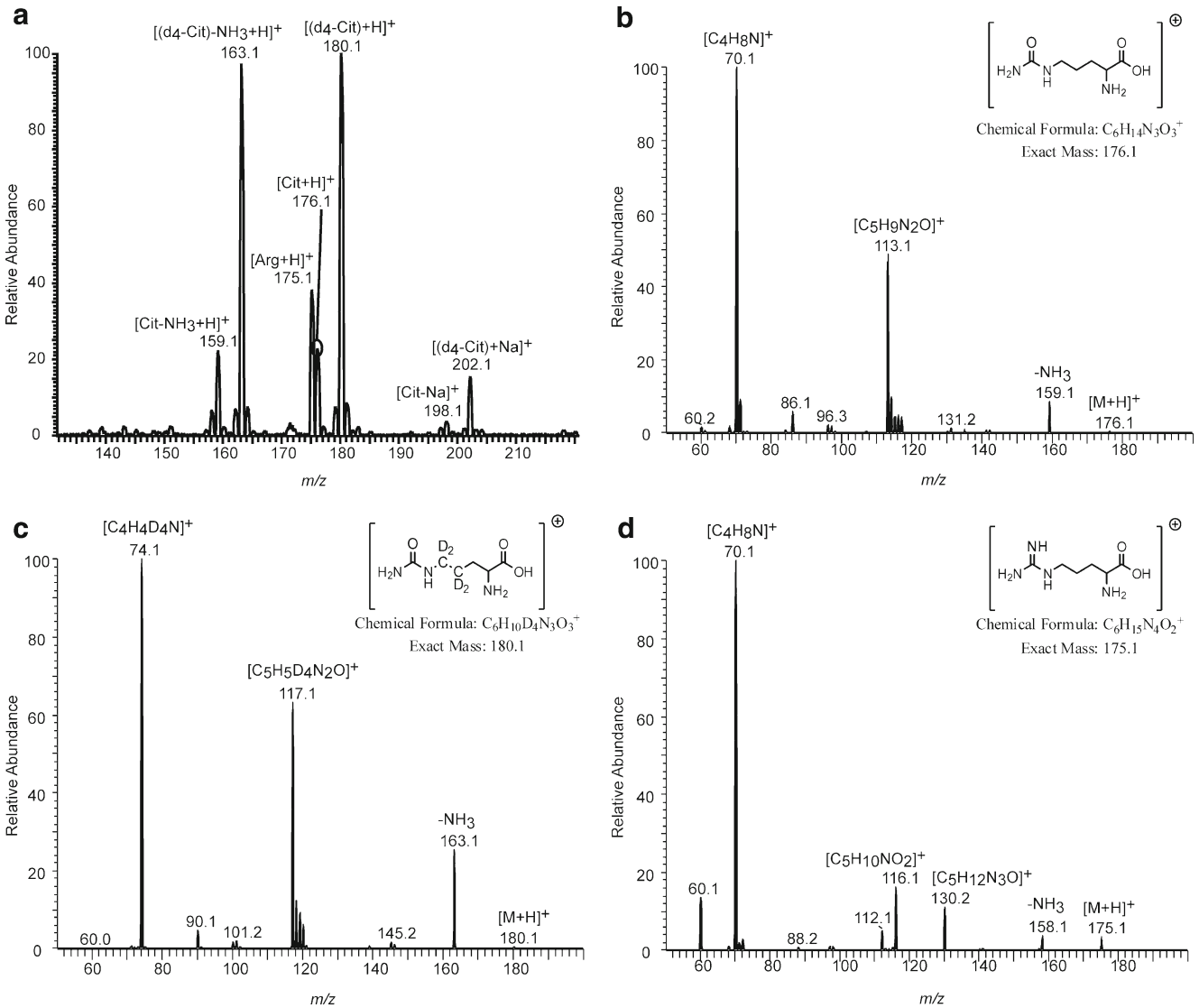

Fig. 1 Mass spectrum and tandem mass spectra of Cit, d_4-Cit, and Arg. (**a**) Mass spectrum of Cit, d_4-Cit, and Arg. The precursor ions at *m/z* values 175.1, 176.1, and 180.1 were identified as protonated Arg, Cit, and d_4-Cit, respectively. Sodium adducts were also present for these analytes. In addition to the protonated ions for Cit and d_4-Cit, there were also abundant ions, *m/z* 159.1 and *m/z* 163.1, corresponding to the neutral loss of ammonia (NH_3) from these protonated ions, respectively. (**b**) Tandem mass spectrum of Cit. (**c**) Tandem mass spectrum of d_4-Cit. (**d**) Tandem mass spectrum of Arg. Tandem mass spectra were recorded using relative high-collision energy resulting in the most abundant product ion being the protonated pyrroline, *m/z* 70.1 for Cit and Arg and *m/z* 74.1 for d_4-Cit. Conversely, when relative low collision energy was employed the most abundant product ion observed was the neutral loss NH_3, *m/z* 159.1 for Cit, *m/z* 158.1 for Arg, and *m/z* 163.1 for d_4-Cit (data not shown). Molecular formulas for product ions were based on literature [34, 35] and represent the most likely structure assignment from gas-phase fragmentation of the protonated amino acids

scan mass spectrum. This decision was further justified based on consistent measurement of Cit from blood plasma that resulted in acceptable and consistent limits of detection and quantitation across our radiation animal models (*vide infra*).

The three most abundant product ions resulting from the gas-phase dissociation of the Cit precursor ion (*m/z* 176.1) were *m/z* values of 70.1 (high collision energy; Fig. 1b), 113.1 (high collision energy; Fig. 1b) and 159.1 (low collision energy, data not shown). Previous reports for Cit detection and quantitation have utilized SRM transitions of *m/z* 176.1→70.1, 176.1→113.1, 176.1→159.1 [22–28]. Of note, Demacker et al. used the transition *m/z* 176.1→70.1 for quantitation and the transition 176.1→113.1 for qualification and Brown et al. used both transitions (176.1→70.1 and 176.1→113.1) for quantitation. The use of multiple *m/z* transitions greatly increases the selectivity of the detection assay and is highly preferable for assays involving low molecular weight analytes particularly for those analytes that have common structural features [32, 33]. We evaluated the use of three single *m/z* transitions ((1) 176.1→70.1, (2) 176.1→113.1, and (3) 176.1→159.1) and the use of two simultaneous transitions from the combination of the three single transitions ((4) 176.1→70.1 and 176.1→113.1, (5. 176.1→70.1 and 176.1→159.1, and (6) 176.1→113.1 and 176.1→159.1). The use of two simultaneous *m/z* transitions for Cit detection and quantitation involves detection of Cit only if both *m/z* transitions are met. This detection scheme is different than the use of the one transition for qualification and one transition for quantitation. The use of two simultaneous transitions increases the selectivity of the detection scheme by increasing the threshold for analyte detection (i.e., requirement of two *m/z* transitions to be satisfied as opposed to one *m/z* transition). As described below for Cit detection and quantitation, the increased selectivity of two simultaneous transitions also corresponded to increased sensitivity. Linear regression calibration curves were determined for the six *m/z* transitions (see Electronic supplementary material Fig. S1). The slope of the linear regression line directly corresponded to the sensitivity of the curve. The linear regression line was calculated by plotting the area ratio of Cit to d_4-Cit versus the concentration. A steeper slope corresponded to a greater ratio of Cit to d_4-Cit per designated concentration value. The d_4-Cit concentration was kept constant so the only variable was the calculated Cit area per *m/z* transition. A comparison of the slopes for the six *m/z* transitions demonstrated the transition pair of *m/z* 176.1→70.1 and 176.1→159.1 had the steepest slope and therefore had the most sensitivity (Electronic supplementary material Table S1). Of major note, sensitivity was not the only consideration for choosing a *m/z* transition. Equally important was the selection of a *m/z* transition that is highly selective to the analyte of interest. As mentioned above, the choice of selecting a labile and common neutral loss (NH_3) for a single *m/z* transition is not recommended, yet its choice in a transition pair was justified by the combined selectivity of the transition pair and its sensitivity over the other transitions. The selectivity of the *m/z* transition pair 176.1→70.1 and 176.1→159.1 was demonstrated across the radiation animal models as detailed below. SRM transitions for d_4-Cit and Arg were as follows: *m/z* 180.1→74.1 and *m/z* 175.1→70.1, which were consistent with literature [22, 23, 27, 28].

Chromatographic separation Cit, d_4-Cit and Arg were separated from other matrix components using a core-shell unbonded silica HILIC column. HILIC columns are advantageous for separating polar molecules such as amino acids. Core-shell particle stationary phases have increased chromatographic efficiency owing to their reduced diffusion path length. This particular column chemistry has been demonstrated in literature to provide good chromatographic separation for detection of Cit from plasma [22, 23, 25, 27]. The elution was performed by using a gradient of aqueous buffer (10 mM of ammonium formate with 0.1 % FA) in ACN (0.1 % FA). The total chromatographic run time was 6.0 min. Cit and d_4-Cit coeluted at a retention time of 3.12 min and Arg eluted at a retention time of 3.30 min (Fig. 2). This provided baseline separation for Cit and Arg.

Arg was included in the assay for detection of Cit for the following several reasons: first, endogenous Arg is present in plasma at high concentrations (>100 μM) [13, 22, 23]; secondly, Arg had a similar chromatographic retention time to Cit (Cit t_r=3.12 min; Arg t_r=3.30 min); and lastly, Arg and Cit's most abundant SRM transition is nearly identical (Cit (*m/z* 176.1→70.1), Arg (*m/z* 175.1→70.1)). Most importantly, the chromatographic conditions employed here provided baseline separation of Cit and Arg. Baseline separation for Cit and Arg was achieved for all six *m/z* transitions evaluated in the previous section (Fig. 2). All Cit *m/z* transitions were not completely unique to Cit as evident of the additional chromatographic peak with varying abundance at the Arg retention time of 3.30 minutes. Arg interference was assessed by determining the amount of Arg present for each Cit *m/z* transition. This was accomplished by preparing Cit standard curves spiked with d_4-Cit (internal standard) and Arg at 200 uM for each Cit *m/z* transition. Then, the ratio of Cit to Arg was calculated after normalizing to the internal standard d_4-Cit. The results showed that the most selective *m/z* transition in the context of interfering Arg was *m/z* 176.1→159.1 (Electronic supplementary material Table S2). Although the *m/z* 176.1→159.1 transition was most selective, for the reasons mentioned above, the use of a single *m/z* transition using a common, labile neutral loss is widely discouraged. Additionally, selection of a *m/z* transition does not only involve consideration of the transition's selectivity. In this case, there was chromatographic baseline resolution between Cit and Arg, and as such,

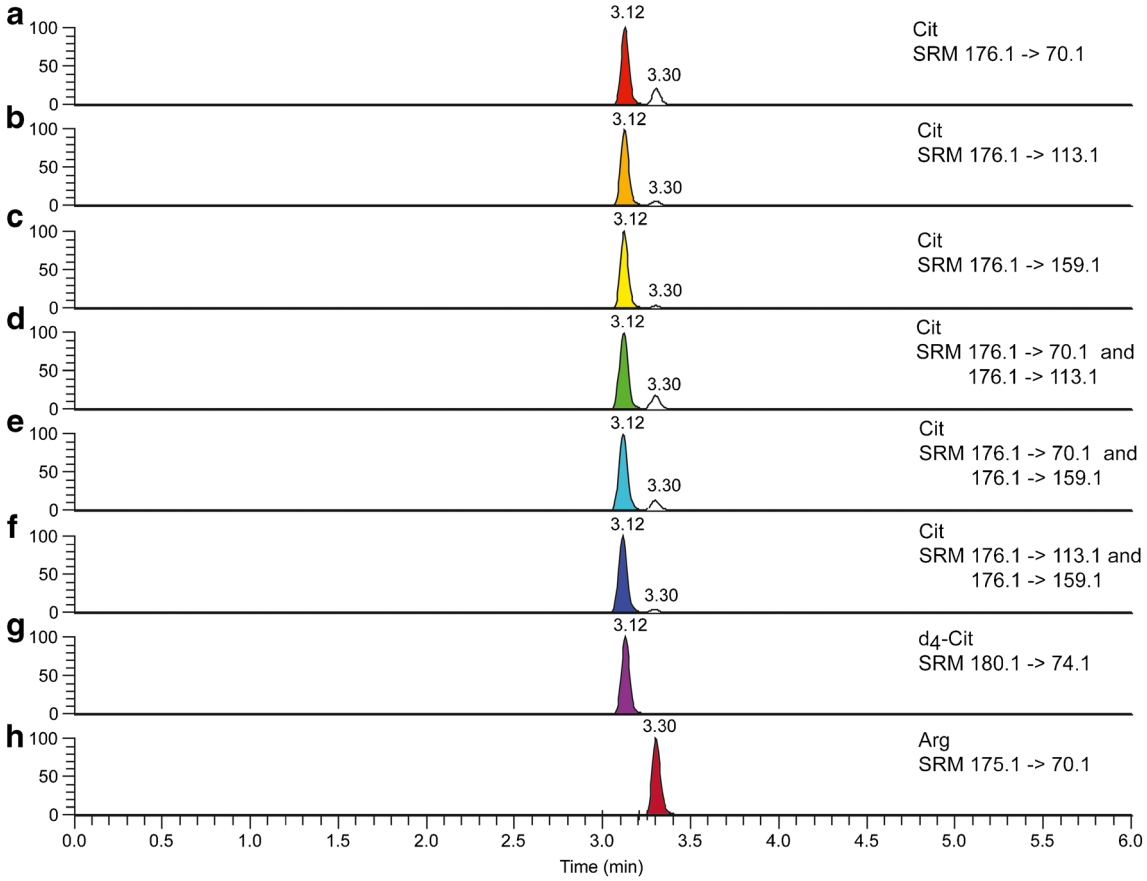

Fig. 2 Total ion chromatograms (TICs) for Cit (six different *m/z* transitions), d_4-Cit, and Arg from spiked neat standards. (**a**) Cit SRM chromatogram for transition *m/z* 176.1→70.1. (**b**) Cit SRM chromatogram for transition *m/z* 176.1→113.1. (**c**) Cit SRM chromatogram for transition *m/z* 176.1→159.1. (**d**) Cit SRM chromatogram for transition *pair m/z* 176.1→70.1 and *m/z* 176.1→113.1. (**e**) Cit SRM chromatogram for transition pair *m/z* 176.1→70.1 and *m/z* 176.1→159.1. (**f**) Cit SRM chromatogram for transition pair *m/z* 176.1→113.1 and *m/z* 176.1→159.1. (**g**) d_4-Cit SRM chromatogram for transition *m/z* 180.1→74.1. (**h**) Arg SRM chromatogram for transition *m/z* 175.1→70.1. Note, quantitation not only involved the peak area associated with the peak at retention time 3.12 and excluded the peak area for peak at retention time 3.30

selectivity was considered important yet it was not the only consideration for selecting the most appropriate *m/z* transition. Furthermore, the use of multiple transitions, in our case two, is intrinsically more selective than a single transition especially when considering the possibility of other interferences besides Arg.

Based on balancing both sensitivity and selectivity we determined the most appropriate *m/z* transition pair for Cit detection and subsequent quantitation from blood plasma was the *m/z* transition pair of *m/z* 176.1→70.1 and *m/z* 176.1→159.1 which was the most sensitive transition pair and the second most selective transition pair in the context of Arg interference (Electronic supplementary material Table S2).

Method validation

Specificity Specificity was demonstrated via a unique SRM transition pair for detection and via robust, reproducible chromatographic separation. Cit is an endogenous substance in animal plasma and consequently Cit free plasma is not a readily accessible option. We evaluated Cit specificity in our assay by comparing spiked Cit, d_4-Cit, and Arg in neat standards; spiked Cit, d_4-Cit, and Arg in plasma samples; and endogenous Cit and Arg with spiked d_4-Cit in plasma samples. Plasma from humans, mice, and NHPs were used for specificity evaluation. Figures 2 and 3 display Cit, d_4-Cit, and Arg SRM chromatograms for neat standards and endogenous Cit and Arg in NHP plasma samples, respectively. Comparison of SRM chromatograms from neat standards (Fig. 2), spiked plasma (data not shown), and endogenous plasma (Fig. 3) revealed no significant interference from coeluting substances and the retention times for all target analytes were consistent across the three prepared sample preparations. As detailed above, the assay employed herein provided baseline separation between Cit and Arg and no other noteworthy peaks were present for the Cit SRM transitions used for detection. Therefore, it was demonstrated that our present LC-MS/MS assay was suitable for detection of Cit from plasma.

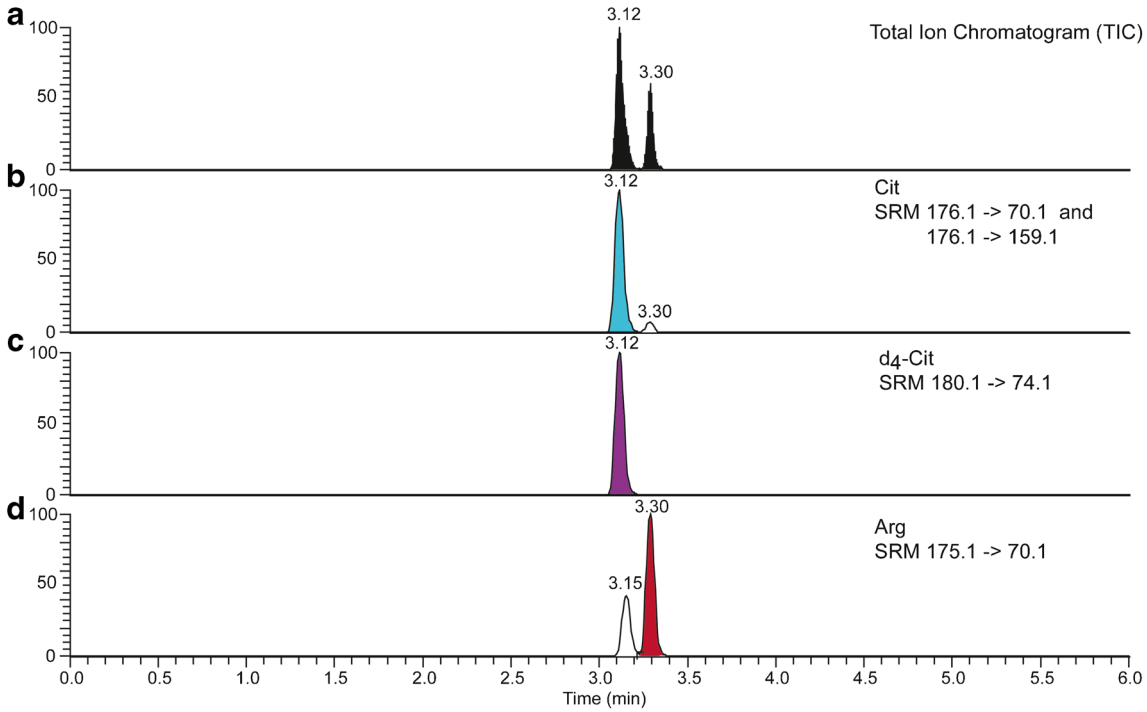

Fig. 3 TICs for Cit, d_4-Cit, and Arg for endogenous Cit and Arg with spiked d_4-Cit from NHP plasma. (**a**) TIC for all SRM transitions: *m/z* 175.1→70.1; *m/z* 176.1→70.1 and *m/z* 176.1→159.1; and *m/z* 180.1→74.1. (**b**) Cit SRM chromatogram for transition pair *m/z* 176.1→70.1 and *m/z* 176.1→159.1. (**c**) d_4-Cit SRM chromatogram for transition *m/z* 180.1→74.1. (**d**) Arg SRM chromatogram for transition *m/z* 175.1→70.1. Note, quantitation for Cit only involved the peak area associated with the peak at retention time 3.12 and excluded the peak area for peak at retention time 3.30

Linearity The establishment of robust calibration curves for endogenous metabolites that have no true blank matrix is challenging. Several approaches have been utilized with varying success. Neat standard calibration curves using the stable-label isotope method are the first approach for method development to ensure practicality and feasibility. The introduction of a stable-label isotope can compensate for matrix effects and extraction efficiency. Comparatively, the use of background subtraction techniques during data processing, where the matrix containing endogenous levels of the analyte of choice are spiked with exogenous levels of the analyte and a corresponding stable-label isotope, provide one-to-one correlation of the target analyte across the sample matrix but are challenging due to the variability of the endogenous concentration among individual samples. A third method, termed the surrogate analyte approach, involves the use of a stable-label isotope of the analyte as a surrogate standard [36]. Calibration curves are generated by adding varying concentrations of the stable-label isotope surrogate standard, addition of a second stable-label isotope standard as an internal standard to the sample matrix followed by sample extraction. The drawbacks with this approach are the expense incurred for two stable-label isotope standards and the verification that the surrogate standard reliably mimics the target analyte in terms of extraction and ionization efficiencies.

The quantitation of Cit from plasma has been achieved using all three of the above methods [22–28] yet, to date, there has not been an evaluation of the different quantitation methods using a tandem quadrupole mass spectrometer as applied to radiation animal models. Of note, Gupta et al. used the spiked plasma and the surrogate analyte approach via the use of a quadrupole time-of-flight (Q-TOF) mass spectrometer and determined the surrogate analyte approach was sufficiently validated in multiple animal species. The use of Q-TOF mass spectrometers or alternative high-resolution mass spectrometers (HRMS) for small molecule quantitation is becoming more common with near comparable sensitivity and selectivity performance to that of tandem quadrupole quantitation [37]. However, the present advantages tandem quadrupole quantitation affords including operational expenses, better sensitivity and greater linear range, and general market availability make the use of a validated tandem quadrupole quantitation assays more practical and readily available for a general audience.

Seven point calibration curves were generated for Cit from neat standards, spiked plasma samples using background subtraction, and the surrogate analyte method. Each calibration curve was generated using the stable-label isotope or surrogate analyte method followed by application of a linear least-squares regression analysis [38]. The stable-label isotope method involved the use of d_4-Cit as the internal standard.

The surrogate analyte method involved the use of the surrogate analyte of ^{13}c-Cit and ^{13}c-d_4-Cit as the internal standard. The *m/z* transition pair for ^{13}c-Cit was *m/z* 177.1→70.1 and 177.1→160.1 and the *m/z* transition for ^{13}c-d_4-Cit was *m/z* 181.1→75.1. The Cit calibration curves were validated over the range of 0.1–200 μM for neat standards and 1–200 μM for plasma standards. Plasma standard calibration curves were determined by applying background subtraction to compensate for endogenous Cit in plasma. The background subtraction was calculated by taking the mean value of Cit to d_4-Cit area ratio for five independent samples per plasma matrix. All calibration curves were linear with correlation coefficients of >0.995. Representative calibration curves and linear regression equations are displayed in Electronic supplementary material Fig. S2 and Table S3. The slopes of the calibration curves (coefficient of variation (CV) was 7.5 %) were all similar among the different matrices and different quantitation methods indicating all three quantitation methods compensated for the matrix effects during quantitation. Plasma citrulline levels from biological samples were demonstrated to be highly comparable with a CV of 5.7 % between the three quantitation methods (Electronic supplementary material Table S4). The stable-label isotope method with neat standards and validation via multispecies spiked Cit plasma was chosen based on its comparable performance with the other two quantitation methods (background subtraction and surrogate analyte approach) and its relative ease of sample preparation, the required concentration range in plasma (1–200 μM), LLOQ (1 μM) needed for biological application, and the end product of validating our approach with quality control samples across species and consistent Cit concentrations to reported literature. Basal concentration of plasma citrulline for human plasma was 31.3±2.2 μM, mouse plasma was 41.6±1.8 μM, and NHP plasma was 40.5±1.7 μM. Citrulline values were calculated from five independent biological sources for the human and mouse measurements and 36 independent biological sources for the NHP measurements. The results are reported as mean±SEM. These values were highly comparable to the literature [22–28].

Lower limit of quantitation, accuracy, and precision The LLOQ was set at the concentration of 1 μM representing the lowest value on the plasma calibration curves. The LLOQ was evaluated across the matrix platform (neat standards and human, mouse, and NHP plasma) on three independent batches of $n=5$ per matrix. Accuracy and intra- and interday precision were evaluated by analysis of five quality control samples at low (5 μM), middle (50 μM), and high (100 μM) concentration levels of spiked Cit in neat solution and in plasma from the three species. The criteria threshold for accuracy and precision were ±20 % of nominal value and less than 15 % CV, respectively. Intraday experiments consisted of analysis of QC samples within an 8-h time period and interday experiments consisted of analysis of the QC samples over a 3-day interval. Refer to Table 2 for LLOQ, accuracy, and precision values.

Extraction recovery and matrix effects Analyte extraction recovery and matrix effects were evaluated based on the methods proposed by Chambers et al. [39] and Wang et al. [23]. The extraction recovery was calculated by dividing the mean peak area of Cit ($n=5$) from plasma samples spiked prior to extraction from plasma samples spiked post extraction. The matrix effect was calculated by dividing the mean peak area of Cit ($n=5$) from plasma samples spiked post extraction from spiked neat solution samples. Equivalent low, medium, and high concentration QC samples were used for all extraction recovery and matrix effect experiments. Cit extraction recovery for low, medium, and high QC samples was consistent per matrix. The mean extraction recovery (reported in %) for human, mouse, and NHP plasma extracts were 64.0±5.1, 74.4±4.4, and 69.1±4.8, respectively. The mean matrix effects (reported in %) for Cit were 83.4±6.4 for human, 86.6±3.8 for mouse, and 85.2±4.9 for NHP.

Stability Stability under sample collection and storage were evaluated by freeze–thaw stability, short-term temperature stability, and postpreparative stability experiments. Plasma samples from each species were subjected to three freeze–thaw stability cycles. The freeze–thaw cycle involved freezing samples at −80 °C, and then thawing unassisted under ambient room temperature conditions. There were no significant ($p>0.05$) decrease in the peak area response for Cit for the duration of the freeze–thaw stability experiment for all three species. Short-term (bench-top) stability temperature was accessed by determining the concentration of Cit extracted from plasma before and after exposure to 2 h at room temperature. The mean percentage difference for all species at $n=5$ was less than 0.5 %. Lastly, postpreparative stability was evaluated at time points 8, 24, and 48 h at room temperature (bench-top) and 4 °C (auto-sampler). The mean percentage difference for Cit values from the room temperature experiments were <1.0, <3.5, and <5.2 % for 8, 24, and 48 h, respectively. The mean percentage difference for Cit values at 4 °C were <1.0 % for 8 and 24 h and <2.6 % for 48 h. No significant differences ($p>0.05$) were observed between species for any of the stability experiments.

Determination of Citrulline quantitation in plasma from animal models of GI-ARS The assay developed herein was applied to quantitation of Cit from plasma samples that were obtained from animal models of radiation-induced GI-ARS. The radiation animal models included the following species: mice, minipigs, and NHP. Of particular note, we analyzed 36 independent NHP plasma samples in order to establish the

Table 2 LLOQ, intraday, and interday accuracy and precision for quantitation of citrulline from neat solution and plasma from human, mouse, and NHP

	Matrix											
		Neat solution			Human			Mouse			NHP		
	Nominal (μM)	Mean (μM)	SD	CV (%)	Mean (μM)	SD	CV (%)	Mean (μM)	SD	CV (%)	Mean (μM)	SD	CV (%)
LLOQ	1	1.0	0.1	4.9	1.1	0.1	7.0	1.0	0.1	3.9	1.0	0.1	4.9
Intraday accuracy and precision	5	5.9	0.2	3.4	5.4	0.3	5.5	5.7	0.2	4.1	5.6	0.3	4.4
	50	49.8	1.8	3.6	49.4	2.9	5.9	53.9	1.8	2.1	53.7	2.5	4.7
	100	100.1	3.2	3.2	84.0	5.1	6.1	91.0	4.0	4.4	87.1	4.2	4.8
Interday accuracy and precision	5	6.0	0.3	4.2	5.8	0.3	5.1	5.7	0.3	4.4	5.5	0.3	5.1
	50	52.1	2.2	4.2	54.5	3.1	5.7	56.0	2.0	3.5	50.1	2.6	5.2
	100	111.6	4.8	4.3	94.4	5.3	5.6	94.1	4.2	4.4	88.6	4.3	4.9

Concentrations are reportedin μM with n=5 per matrix

SD standard deviation, *CV* coefficient of variation, *LLOQ* lower limit of quantitation

baseline plasma citrulline levels for NHPs (Fig. 4). The mean ±SEM was 40.5±1.7 μM, CV was 24.8 %, and minimum/maximum values of 26.1 and 65.7 μM, respectively.

In order to validate the developed assay of measuring circulating Cit concentrations within the context of these radiation animal models we chose a dose of total-body irradiation (TBI) associated with the GI-ARS in each species. Mice, minipig or NHP were exposed to 13, 10, and 10.5 Gy TBI, respectively. Several early time points were chosen for each species from days 1 to 7 post-TBI. Samples from non-irradiated animals were included as controls and designated as day 0. Day 0 plasma samples were obtained from the individual animal in the case of the minipig and NHP experiments and from age-matched controls for the mice experiments. Mouse blood was collected upon euthanasia due to volume and ease of collecting blood. Day 0 plasma samples were taken prior to irradiation. A minimum of three biological replicates were evaluated per dose per time point. Figure 5 displays the graphical representation of circulating citrulline concentration in micromolar or I prefer to use μM (mean±SEM) as a function of time post-irradiation for the mouse, minipig, and NHP models. Figure 5a represents plasma citrulline concentrations from mice exposed to 13 Gy TBI for days 1 to 6 post-irradiation. Plasma citrulline concentrations from minipigs exposed to 10 Gy TBI for time points 1, 2, 3, and 7 days post-irradiation are displayed in Fig. 5b. Figure 5c represents plasma citrulline concentrations from NHPs exposed to 10.5 Gy TBI for time points 1, 3, 5, and 7 days post-irradiation.

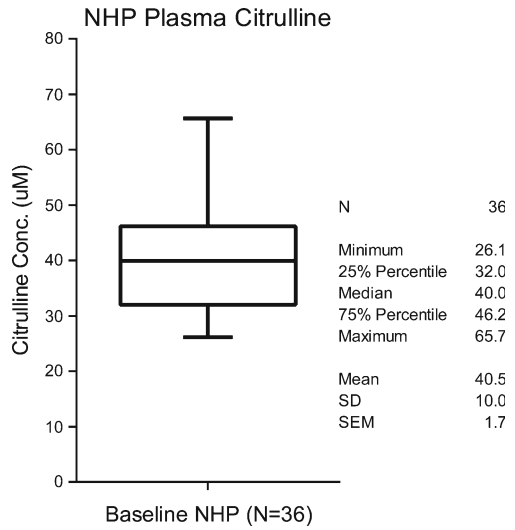

Fig. 4 Box plot representation of NHP plasma citrulline sampled from 36 independent sources. The mean±SEM was 40.5±1.7. The minimum value was 26.1 and the maximum value was 65.7. Concentrations are reported in μM. *N* number of independent plasma sources, *SD* standard deviation, *SEM* standard error of the mean, *CV* coefficient of variation

Discussion

Herein, we present the development and validation of a LC-MS/MS assay for the quantitation of citrulline from plasma samples derived from three animal species, the mouse, minipig, and NHP. The main charge for developing this assay was to assess the legitimacy of circulating citrulline as a biomarker for GI-ARS. A number of reports have linked plasma citrulline to small intestine function [3–8], yet to date there has not been a conclusive report using well-characterized animal models of the acute GI-ARS for establishing citrulline as a *bona fide* biomarker of GI-ARS. Prior to a comprehensive evaluation of plasma citrulline as a biomarker for GI-ARS, we first set about to establish a validated quantitation assay for plasma citrulline using radiation animal models and following strict adherence to the FDA's Guidance for Industry, Bioanalytical Methods Validation.

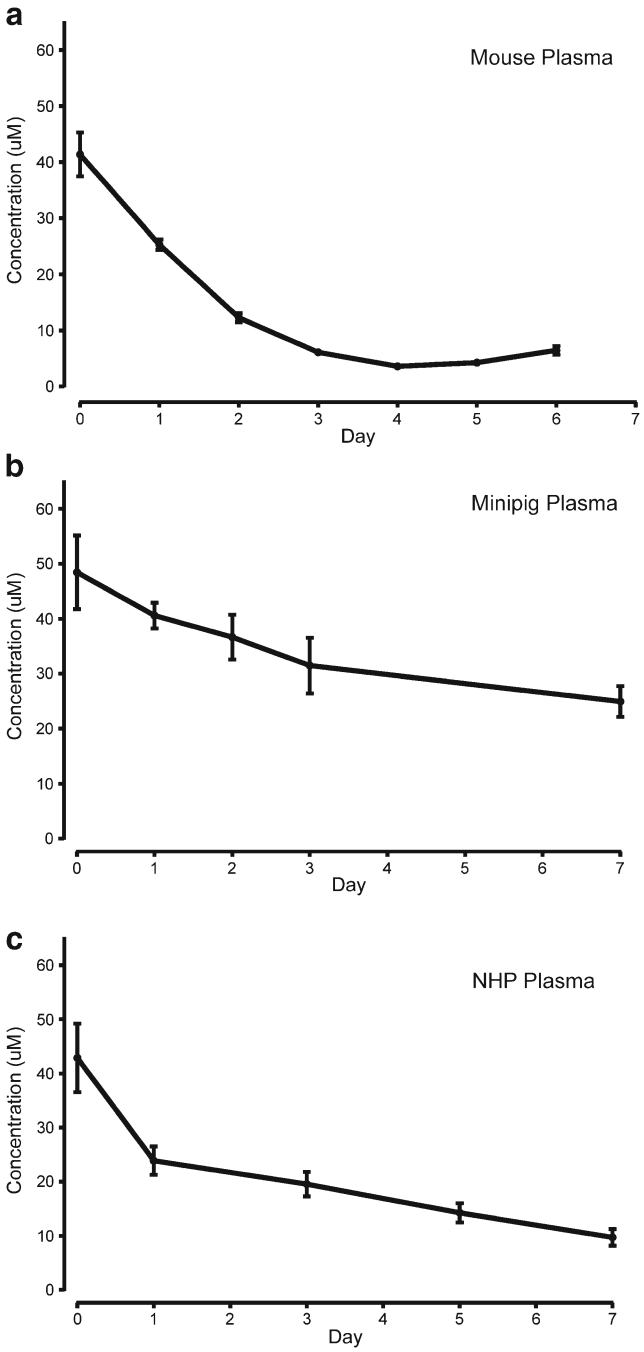

Fig. 5 Circulating citrulline concentration (μM) as a function of time post-TBI. (**a**) Mouse plasma citrulline expressed as a function of time post-TBI at 13 Gy. Citrulline concentration was reported as mean±SEM. There were five biological replicates for days 0–4 and four biological replicates for days 5 and 6. (**b**) Minipig plasma citrulline expressed as a function of time post-TBI at 10 Gy. Citrulline concentration was reported as mean±SEM. There were three biological replicates for per time point. (**c**) NHP plasma citrulline expressed as a function of time post-TBI at 10.5 Gy. Citrulline concentration was reported as mean±SEM. There were four biological replicates for per time point

The assay was developed using plasma samples from human, mouse, and NHP subjects. Mouse and NHP plasma were chosen because these two species represent the small and large animal radiation models that will be used by the Medical Counter Measures Against Radiological Threats (MCART) consortium for comprehensive evaluation of plasma citrulline as a biomarker for the acute GI-ARS. In addition, we included the use of human plasma samples for method development and validation owning to the prospective translation of citrulline as a biomarker for GI-ARS in humans. Assay specificity, linearity, LLOQ, accuracy, precision, extraction recovery, matrix effects, and stability under sample collection and storage were all assessed for plasma samples from human, mouse, and NHP. In particular, detection and quantitation was evaluated across six different *m/z* transitions and three different quantitation methods. To date, systematic evaluation of the sensitivity and selectivity of six *m/z* transitions or comparison of multiple quantitation methods using the standard tandem quadrupole mass spectrometry platform has not been described. It was determined that the most sensitive and selective *m/z* transition involved the use of the two simultaneous transitions of *m/z* 176.1→70.1 and *m/z* 176.1→159.1. The preferred quantitation method utilized the benchmark stable-label isotope method validated in neat standards and multiple animal plasma samples.

The LC-MS/MS platform provided high selectivity in the form of rapid, efficient HILIC separation and a unique SRM transition pair. In addition, the assay provided sufficient sensitivity to reach 1 μM LLOQ in plasma for all animal species. The 1-μM LLOQ was deemed appropriate for citrulline quantitation from plasma for the animal models based on a previous report where it was demonstrated that citrulline plasma concentrations for high-dose irradiation over the GI-ARS of mice reached its nadir at 3 μM [40]. Accuracy and precision was consistent and robust across the three species with the highest variation occurring at the 5-μM QC sample for all three species. In addition, human plasma displayed the most variation presumably because the human diet and lifestyle is the least constant amongst the animal populations studied here, whereas, mice and NHPs have consistent diets and health care monitoring throughout for the duration of the experiments. The human plasma samples were obtained from a blood bank where correlation to the individual's "lifestyle" was unavailable. Circulating citrulline is known to be dependent on age, disease, and fasting which could explain the increased variability of the human plasma samples [9, 10, 41]. In humans, plasma citrulline levels for normal healthy adults is 40±10 μM with a suggested clinical range of 20 to 60 μM [9, 42]. To this end, plasma samples from 36 independent NHPs were analyzed for determining the baseline levels of plasma citrulline for NHPs. It was determined that the plasma citrulline levels for healthy NHP adults were 40.5± 1.7 μM with a range of 26.1 and 65.7 μM, which were highly comparable to the reported normal healthy human plasma citrulline levels. The NHP plasma citrulline values reported

herein were similar to literature [25, 43, 44], yet the values in literature were taken from small sample sizes ranging from two to four individual sources. The determination of baseline NHP plasma citrulline from 36 independent sources represented the most comprehensive and robust analysis of plasma citrulline from NHPs to date. The establishment of baseline NHP plasma citrulline from a large sample size is a very important benchmark for validating citrulline as a biomarker for GI-ARS within in the NHP radiation animal model.

The evaluation of matrix effects and extraction recovery are crucial parameters that need to be verified when developing an LC-MS/MS assay [45]. Matrix effects and extraction recovery can severely impair selectivity and sensitivity for LC-MS/MS assays and can vary depending on sample preparation and sample matrix. We elected for a simple, rapid sample preparation procedure of organic protein precipitation. This sample preparation procedure, although very common due to its ease of use and low cost, is prone to highly variable extraction recovery and matrix effects [46]. Based on the method of Chambers et al. [39], we reported nearly 25–35 % decrease in extraction recovery and approximately 13–18 % matrix effect for citrulline quantitation from plasma across the three species for the organic protein precipitation sample preparation. Extraction recoveries and matrix effects were similar to previous published reports [23–25]. More elaborate and/or expensive sample preparation techniques could have been utilized to improve extraction recovery and minimize matrix effects yet the addition of a stable-label isotope (d_4-Cit) as an internal standard allowed for the use of a quick sample preparation procedure. The addition of the stable-label isotope that was exposed to the same extraction efficiency, chromatographic separation, and ionization suppression yielded a constant analyte to internal standard ratio compensating for extraction recovery and matrix effects.

Next, the application of the validated LC-MS/MS assay was applied to plasma samples from three animal models of acute TBI at doses and time points associated with the GI-ARS. The three models of the acute GI-ARS induced by TBI were the mouse [31], minipig [47], and NHP [48]. Of note, the minipig plasma was not included in the analytical method development and validation. The analytical development and validation was designed to cover the two most common small (mouse) and large (NHP) animal models of the ARS. Moreover, the inclusion of an animal model of acute radiation exposure that was outside of the method development process was considered additional validation of the biological application. The positive confirmation that the developed LC-MS/MS assay for quantitation of plasma citrulline can be applied to animal models of the acute GI-ARS outside of the mouse and NHP further expands its versatility and validity. The importance of assay versatility can be seen in the need for multiple animal models to help characterize and understand radiation injury given the nature of radiation experiments dependence on laboratory animals and not humans [49, 50].

Circulating citrulline concentrations were determined for the mouse, minipig and NHP animal models, over an early time course after a dose of TBI characteristic of the GI-ARS (Fig. 4). What follows was a steady and pseudo-linear decrease in plasma citrulline over time consistent with the progressive effects of inhibited citrulline production in the small intestinal enterocytes. This response was expected and consistent with reports in the literature [25, 40, 43]. A previous report of mice irradiated from 8 to 15 Gy where plasma citrulline was measured at days 4 and 6 post-irradiation not only showed a dose response for citrulline concentration but highlighted time course dependence as well. Additionally, this report compared the histology of the small intestine to plasma citrulline in order to evaluate the link between small intestine structural integrity and plasma citrulline. At 11 Gy, the day 4 pathology assessed via H&E staining displayed noticeable loss of the epithelium consistent with decreased enterocyte function. Accordingly, plasma citrulline was reported to have an approximately 90 % reduction compared with non-irradiated controls. This data suggested the small intestine function and structure parallels plasma citrulline concentration at least for day 4 for 11 Gy. It should be noted that conclusions drawn from this dose and time point need further validation and do not represent initial insult (days 1–3) and recovery (day 4+) if applicable. With the establishment of a validated LC-MS/MS assay for quantitation of plasma citrulline from well-characterized radiation animal models, we now intend, via ongoing efforts, to determine the potential relationship between circulating citrulline concentration and acute and prolonged radiation-induced GI injury.

The potential utility of citrulline or any other biomarker hinges on the establishment of a quantitation assay that has been validated within the framework of its intended use. In the case of biomarkers to be used for developing MCMs to treat high-dose irradiation exposure, the first and most crucial step is validation of the quantitation assay using the exact same radiation animal models that will be used for the MCM pipeline which has been the case for citrulline as detailed herein.

Conclusions

A LC-MS/MS assay for the quantitation of plasma citrulline was developed and validated as prescribed by the FDA's Guidance for Industry, Bioanalytical Methods Validation. Method validation was performed using plasma from human, mouse, and NHP samples. The validated assay was applied to the determination of plasma citrulline from three animal models of the acute GI-ARS including the mouse, minipig, and NHP. Successful application of the citrulline quantitation

assay to well-characterized animal models lays the foundation for incorporating circulating citrulline determination as a potential biomarker for gaining greater understanding of acute and prolonged radiation-induced GI injury, and its potential use as a quantitative readout for efficacy of medical countermeasures to treat individuals following high-dose irradiation exposure.

Acknowledgments This work was funded with Federal funds from the National Institute of Allergy and Infectious Diseases (contract no. HHSN272201000046C). This work is also supported in part by the University of Maryland Baltimore, School of Pharmacy Mass Spectrometry Center (SOP1841-IQB2014). The authors would like to thank all members of the Medical Countermeasures Against Radiological Threats (MCART) consortium for their dedication, support, and guidance in establishing biomarker identification and validation as a priority in the radiation medical counter measure field. Additionally, we would like to acknowledge and thank all members of the Kane laboratory.

References

1. MacVittie TJ (2012) The MCART consortium animal models series. Health Phys 103:340–342. doi:10.1097/HP.0b013e318261175a
2. Potten CS (1990) A comprehensive study of the radiobiological response of the murine (BDF1) small intestine. Int J Radiat Biol 58: 925–973
3. Papadia C, Sherwood RA, Kalantzis C et al (2007) Plasma citrulline concentration: a reliable marker of small bowel absorptive capacity independent of intestinal inflammation. Am J Gastroenterol 102: 1474–1482. doi:10.1111/j.1572-0241.2007.01239.x
4. Lutgens L, Lambin P (2007) Biomarkers for radiation-induced small bowel epithelial damage: an emerging role for plasma citrulline. World J Gastroenterol 13:3033–3042
5. Pappas PA, Saudubray JM, Tzakis AG et al (2001) Serum citrulline and rejection in small bowel transplantation: a preliminary report. Transplantation 72:1212–1216
6. Crenn P, Vahedi K, Lavergne-Slove A et al (2003) Plasma citrulline: a marker of enterocyte mass in villous atrophy-associated small bowel disease. Gastroenterology 124:1210–1219. doi:10.1016/S0016-5085(03)00170-7
7. Cynober L, Melchior JC, Crenn P et al (2009) Plasma citrulline is a biomarker of enterocyte mass and an indicator of parenteral nutrition in HIV-infected patients. Am J Clin Nutr 90:587–594. doi:10.3945/ajcn.2009.27448.INTRODUCTION
8. Rendon JL, Li X, Gupta P et al (2012) Decreased serum citrulline correlates with increased gut permeability following ethanol exposure and burn injury. Alcohol 42:177
9. Rabier D, Kamoun P (1995) Metabolism of citrulline in man. Amino Acids 9:299–316. doi:10.1007/BF00807268
10. Wu G, Knabe DA, Flynn NE (1994) Synthesis of citrulline from glutamine in pig enterocytes. Biochem J 299:115–121
11. Fekkes D, van Dalen A, Edelman M, Voskuilen A (1995) Validation of the determination of amino acids in plasma by high-performance liquid chromatography using automated pre-column derivatization with *o*-phthaldialdehyde. J Chromatogr B Biomed Sci Appl 669: 177–186
12. Sultana H, Onodera R, Or-Rashid MM, Wadud S (2001) Convenient method for the determination of arginine and its related compounds in rumen fluid by reversed-phase high-performance liquid chromatography. J Chromatogr B Biomed Sci Appl 755:321–329. doi:10.1016/S0378-4347(01)00137-2
13. Tsikas D, Teerlink T (2007) HPLC analysis of ADMA and other methylated l-arginine analogs in biological fluids. J Chromatogr B 851:21–29
14. Caussé E, Siri N, Arnal J et al (2000) Determination of asymmetrical dimethylarginine by capillary electrophoresis–laser-induced fluorescence. J Chromatogr B Biomed Sci Appl 741:77–83. doi:10.1016/S0378-4347(00)00034-7
15. Schulze F, Wesemann R, Schwedhelm E, Sydow K, Albsmeier J, Cooke JP, Böger RH (2004) Determination of asymmetric dimethylarginine (ADMA) using a novel ELISA assay. Clin Chem Lab Med 42:1377–1383. doi:10.1515/CCLM.2004.257
16. Mao H, Wei W, Xiong W et al (2010) Simultaneous determination of l-citrulline and l-arginine in plasma by high performance liquid chromatography. Clin Biochem 43:1141–1147
17. Harder U, Koletzko B, Peissner W (2011) Quantification of 22 plasma amino acids combining derivatization and ion-pair LC-MS/MS. J Chromatogr B 879:495–504
18. Casetta B, Tagliacozzi D, Shushan B, Federici G (2000) Development of a method for rapid quantitation of amino acids by liquid chromatography-tandem mass spectrometry (LC-MSMS) in plasma. Clin Chem Lab Med 38:391–401. doi:10.1515/CCLM.2000.057
19. Kato M, Kato H, Eyama S, Takatsu A (2009) Application of amino acid analysis using hydrophilic interaction liquid chromatography coupled with isotope dilution mass spectrometry for peptide and protein quantification. J Chromatogr B 877: 3059–3064
20. Thiele B, Füllner K, Stein N et al (2008) Analysis of amino acids without derivatization in barley extracts by LC-MS-MS. Anal Bioanal Chem 391:2663–2672. doi:10.1007/s00216-008-2167-9
21. Qu J, Wang Y, Luo G et al (2002) Validated quantitation of underivatized amino acids in human blood samples by volatile ion-pair reversed-phase liquid chromatography coupled to isotope dilution tandem mass spectrometry. Anal Chem 74:2034–2040. doi:10.1021/ac0111917
22. Brown CM, Becker JO, Wise PM, Hoofnagle AN (2011) Simultaneous determination of 6 L-arginine metabolites in human and mouse plasma by using hydrophilic-interaction chromatography and electrospray tandem mass spectrometry. Clin Chem 57:701–709. doi:10.1373/clinchem.2010.155895
23. Wang H-Y, Hu P, Jiang J (2010) Rapid determination of underivatized arginine, ornithine, citrulline and symmetric/asymmetric dimethylarginine in human plasma by LC-MS. Chromatographia 71:933–939. doi:10.1365/s10337-010-1535-8
24. Jaisson S, Gorisse L, Pietrement C, Gillery P (2012) Quantification of plasma homocitrulline using hydrophilic interaction liquid chromatography (HILIC) coupled to tandem mass spectrometry. Anal Bioanal Chem 402:1635–1641. doi:10.1007/s00216-011-5619-6
25. Gupta PK, Brown J, Biju PG et al (2011) Development of high-throughput HILIC-MS/MS methodology for plasma citrulline determination in multiple species. Anal Methods 3:1759–1768. doi:10.1039/c1ay05213f
26. Demacker PNM, Beijers AM, van Daal H et al (2009) Plasma citrulline measurement using UPLC tandem mass-spectrometry to determine small intestinal enterocyte pathology. J Chromatogr B 877: 387–392
27. Shin S, Fung S-M, Mohan S, Fung H-L (2011) Simultaneous bioanalysis of L-arginine, L-citrulline, and dimethylarginines by LC-MS/MS. J Chromatogr B Analyt Technol Biomed Life Sci 879: 467–474. doi:10.1016/j.jchromb.2011.01.006
28. Martens-Lobenhoffer J, Bode-Böger SM (2003) Simultaneous detection of arginine, asymmetric dimethylarginine, symmetric dimethylarginine and citrulline in human plasma and urine applying

liquid chromatography–mass spectrometry with very straightforward sample preparation. J Chromatogr B 798:231–239. doi:10.1016/j.jchromb.2003.09.050
29. Naidong W, Shou W, Chen Y-L, Jiang X (2001) Novel liquid chromatographic–tandem mass spectrometric methods using silica columns and aqueous–organic mobile phases for quantitative analysis of polar ionic analytes in biological fluids. J Chromatogr B Biomed Sci Appl 754:387–399. doi:10.1016/S0378-4347(01)00021-4
30. Federal Drug Administration (2001) Guidance for industry bioanalytical method validation guidance for industry bioanalytical method validation
31. Booth C, Tudor G, Tudor J et al (2012) Acute gastrointestinal syndrome in high-dose irradiated mice. Health Phys 103:383–399. doi:10.1097/HP.0b013e318266ee13
32. Kushnir MM, Rockwood AL, Nelson GJ et al (2005) Assessing analytical specificity in quantitative analysis using tandem mass spectrometry. Clin Biochem 38:319–327. doi:10.1016/j.clinbiochem.2004.12.003
33. Vogeser M, Seger C (2010) Pitfalls associated with the use of liquid chromatography-tandem mass spectrometry in the clinical laboratory. Clin Chem 56:1234–1244. doi:10.1373/clinchem.2009.138602
34. Dookeran N (1996) Fragmentation reactions of protonated-amino acids. J Mass Spectrom 31:500–508
35. Gogichaeva NV, Williams T, Alterman MA (2007) MALDI TOF/TOF tandem mass spectrometry as a new tool for amino acid analysis. J Am Soc Mass Spectrom 18:279–284. doi:10.1016/j.jasms.2006.09.013
36. Li W, Cohen LH (2003) Quantitation of endogenous analytes in biofluid without a true blank matrix. Anal Chem 75:5854–5859. doi:10.1021/ac034505u
37. Rousu T, Tolonen A (2012) Comparison of unit resolution SRM and TOF-MS at 12,000 mass resolution for quantitative bioanalysis of 11 steroids from human plasma. Bioanalysis 4:555–563. doi:10.4155/bio.11.289
38. Ciccimaro E, Blair IA (2010) Stable-isotope dilution LC-MS for quantitative biomarker analysis. Bioanalysis 2:311–341. doi:10.4155/bio.09.185
39. Chambers E, Wagrowski-Diehl DM, Lu Z, Mazzeo JR (2007) Systematic and comprehensive strategy for reducing matrix effects in LC/MS/MS analyses. J Chromatogr B 852:22–34
40. Jones JW, Scott AJ, Tudor G et al (2014) Identification and quantitation of biomarkers for radiation-induced injury via mass spectrometry. Heal
41. Wakabayashi Y, Yamada E, Hasegawa T, Yamada R (1991) Enzymological evidence for the indispensability of small intestine in the synthesis of arginine from glutamate. Arch Biochem Biophys 291:1–8. doi:10.1016/0003-9861(91)90097-3
42. Crenn P, Messing B, Cynober L (2008) Citrulline as a biomarker of intestinal failure due to enterocyte mass reduction. Clin Nutr 27:328–339. doi:10.1016/j.clnu.2008.02.005
43. Hérodin F, Richard S, Grenier N et al (2012) Assessment of total- and partial-body irradiation in a baboon model: preliminary results of a kinetic study including clinical, physical, and biological parameters. Health Phys 103:143–149. doi:10.1097/HP.0b013e3182475e54
44. Reddy DVN (1967) Distribution of free ammo acids and related compounds in ocular fluids, lens, and plasma of various mammalian species. Invest Ophthalmol 6:478–483
45. Bansal S, DeStefano A (2007) Key elements of bioanalytical method validation for small molecules. AAPS J 9:E109–E114. doi:10.1208/aapsj0901011
46. Jemal M (2000) High-throughput quantitative bioanalysis by LC/MS/MS. Biomed Chromatogr 14:422–429. doi:10.1002/1099-0801(200010)14:6<422::AID-BMC25>3.0.CO;2-I
47. Moroni M, Coolbaugh TV, Mitchell JM et al (2011) Vascular access port implantation and serial blood sampling in a Gottingen minipig (Sus scrofa domestica) model of acute radiation injury. J Am Assoc Lab Anim Sci 50:65–72
48. MacVittie TJ, Farese AM, Bennett A et al (2012) The acute gastrointestinal subsyndrome of the acute radiation syndrome: a rhesus macaque model. Health Phys 103:411–426. doi:10.1097/HP.0b013e31826525f0
49. Williams JP, Brown SL, Georges GE et al (2010) Animal models for medical countermeasures to radiation exposure. Radiat Res 173:557–578. doi:10.1667/RR1880.1
50. Federal Drug Administration (2009) Guidance for industry address efficacy under the animal rule guidance for industry